LAWRENCE
LIVERMORE
NATIONAL
LABORATORY

UCRL-PROC-215983

Soft radiative strength in warm nuclei

A. Schiller, A. Voinov, U. Agvaanluvsan, E. Algin, J. Becker, T. Belgya, L. Bernstein, R. Chankova, P. E. Garrett, M. Guttormsen, G. E. Mitchell, R. O. Nelson, J. Rekstad, S. Siem, A. C. Sunde

October 6, 2005

The International School on Contemporary Physics-III
UlaanBaatar, Mongolia
August 8, 2005 through August 14, 2005

Soft radiative strength in warm nuclei

A. Schiller,[1,2,*] A. Voinov,[3,4] U. Agvaanluvsan,[2,5,6] E. Algin,[2,5,6,7] J. Becker,[2]
T. Belgya,[8] L. Bernstein,[2] R. Chankova,[9] P.E. Garrett,[2,10] M. Guttormsen,[9]
G.E. Mitchell,[5,6] R.O. Nelson,[11] J. Rekstad,[9] S. Siem,[9] and A.C. Sunde[9]

[1]*National Superconducting Cyclotron Laboratory, Michigan State University, East Lansing, Michigan 48824*
[2]*Lawrence Livermore National Laboratory, L-414, 7000 East Avenue, Livermore, California 94551*
[3]*Frank Laboratory of Neutron Physics, Joint Institute of Nuclear Research, 141980 Dubna, Moscow region, Russia*
[4]*Department of Physics and Astronomy, Ohio University, Athens, Ohio 45701*
[5]*North Carolina State University, Raleigh, North Carolina 27695*
[6]*Triangle Universities Nuclear Laboratory, Durham, North Carolina 27708*
[7]*Department of Physics, Osmangazi University, Meselik, Eskisehir, 26480 Turkey*
[8]*Institute of Isotope and Surface Chemistry, Chemical Research Centre HAS, P.O. Box 77, H-1525 Budapest, Hungary*
[9]*Department of Physics, University of Oslo, N-0316 Oslo, Norway*
[10]*Department of Physics, University of Guelph, Guelph, Ontario N1G 2W1 Canada*
[11]*Los Alamos National Laboratory, MS H855, Bikini Atoll Rd., Los Alamos, New Mexico 87545*

We present data on the soft ($E_\gamma < 3$–4 MeV) radiative strength function (RSF) for electromagnetic transitions between warm states (i.e. states several MeV above the yrast line) from two different types of experiments. The Oslo method provides data on the total level density and the sum (over all multipolarities) of all RSFs by sequential extraction from primary-γ spectra. Measurements of two-step-decay spectra following neutron capture yields two-step-cascade (TSC) intensities which are roughly proportional to the product of two RSFs. Investigations on ^{172}Yb and ^{57}Fe have produced unexpected results. In the first case, a strong ($B(M1\uparrow) = 6.5\,\mu_N^2$) resonance at $E_\gamma = 3.3$ MeV was identified. In the second case, a large (more than a factor of 10) enhancement compared to theoretical estimates of the very soft ($E_\gamma \leq 3$ MeV), summed RSF for transitions between warm states was observed. A somewhat weaker (factor ~ 3) enhancement of the RSF in Mo isotopes observed within the Oslo method still awaits confirmation from TSC experiments.

PACS numbers: 23.20.Js, 24.30.Gd, 25.20.Lj, 24.60.Dr

I. INTRODUCTION

Unresolved transitions in the nuclear γ-ray cascade produced in the decay of excited nuclei are best described by statistical concepts: a radiative strength function (RSF) $f_{XL}(E_\gamma)$ for a transition with multipolarity XL and energy E_γ, and a level density $\rho(E_i, J_i^\pi)$ for initial states i at energy E_i with equal spin and parity J_i^π yield the mean value of the partial decay width to a given final state f [1].

$$\Gamma_{if}^{XL}(E_\gamma) = f_{XL}(E_\gamma)\, E_\gamma^{2L+1}/\rho(E_i, J_i^\pi). \qquad (1)$$

Most information about the RSF has been obtained from photon-absorption experiments in the energy interval 8–20 MeV, i.e., for excitations above the neutron-separation energy S_n [2]. Data on the soft ($E_\gamma < 3$–4 MeV) RSF for transitions in the quasicontinuum (several MeV above the yrast line) remain elusive. First data in the statistical regime where obtained from the ^{147}Sm$(n,\gamma\alpha)^{144}$Nd reaction [3]. They indicate a moderate enhancement of the soft $E1$ RSF compared to a Lorentzian extrapolation of the giant electric dipole resonance (GEDR). For spherical nuclei, in the framework of the Fermi-liquid theory, this enhancement is explained by a temperature dependence of the GEDR width [4], the Kadmenskiĭ-Markushev-Furman (KMF) model. However, the experimental technique requires the presence of sufficiently large α widths and depends on estimates of both α and total radiative widths in the quasicontinuum below S_n.

The sequential extraction method developed at the Oslo Cyclotron Laboratory (OCL) [5] has enabled further investigations of the soft RSF by providing unique data for transitions in the quasicontinuum with sufficient averaging. For deformed rare-earth nuclei, it has been shown that the RSF can be described in terms of a KMF GEDR model, a spin-flip giant magnetic dipole resonance (GMDR), and a soft $M1$ resonance [6, 7]. In this work, we report on (i) a strong ($B(M1\uparrow) = 6.5\,\mu_N^2$) resonance at $E_\gamma = 3.3$ MeV in the RSF of ^{172}Yb, (ii) on the first observation of a strong enhancement of the soft RSF in ^{56,57}Fe over model predictions, and (iii) on a similar, albeit weaker enhancement of the soft RSF in a chain of Mo isotopes. Typically, the resonances and enhancements have been observed first by Oslo-type experiments [6, 8, 9] and were investigated further in two-step-cascade (TSC) experiments. In the case of the Mo isotopic chain, only data from Oslo-type experiments are available at present.

In this work, we will first discuss the soft resonance in ^{172}Yb and how its multipolarity can be determined by TSC experiments. Hence, the TSC method will be discussed in more detail there. In the second part of

*Electronic address: schiller@nscl.msu.edu

this work, we discuss the experimental evidence for the strong enhancement of the soft RSF of ^{56,57}Fe by Oslo-type experiments and the confirmation of this observation in a TSC experiment. Again, emphasis is put on the TSC experiment, since with the focus on the possibility of ordering the two involved γ transitions its analysis is done differently than in the first part. In the last part we present data on the weak enhancement of the soft RSF in a chain of Mo isotopes. These results have not yet been confirmed by the TSC method, hence the focus in this part is put on the Oslo-type experiment. The three parts of this paper are also published separately in [7, 9, 10].

II. NATURE OF THE SOFT RESONANCE IN THE RSF OF ^{172}Yb

Mid-shell rare-earth nuclei, due to their high and uniform single-particle level density are well suited objects for statistical spectroscopy. Their RSFs especially for energies below the neutron-separation energy have been investigated for many decades by methods involving neutron capture, most notably by primary γ rays [11]. For deformed rare-earth nuclei, a bump in the total RSF (summed over all multipolarities) around 3 MeV is inferred from total γ spectra [12–14]. In the same region, a concentration of $M1$ strength (scissors mode) is reported in nuclear resonance fluorescence (NRF) experiments [15]. In TSC experiments [16], a connection between these two observations has been made under the assumption of an enhanced scissors mode. However, after 25 years of investigation, the multipolarity of the bump in the RSF is still under debate. $E1$ multipolarity indicates neutron-skin oscillations from which the clearest signal of neutron and proton radii differences could be deduced. $M1$ multipolarity implies evidence of an enhanced scissors mode. The well-tested Oslo method [5] gives accurate data on the level density and total RSF at $E_\gamma \sim$3 MeV. Systematic studies of several rare-earth nuclei have firmly established the bump in the soft RSF [6]. In this work we determine virtually model-independently, the multipolarity of this bump by a newly developed method [17] that combines the results from the Oslo method with an auxiliary TSC experiment.

A. Discussion of the TSC method

The TSC method is based on the measurement of multiplicity-two γ cascades between fixed initial i and final f levels (see, e.g., [16] and references therein). A convenient initial state is that formed in thermal or average resonance capture (ARC); the final state can be any low-lying discrete state. TSC spectra are determined by the branching ratios of the initial and intermediate m states (expressed as ratios of partial to total widths Γ) and by the level density ρ of intermediate states with spin

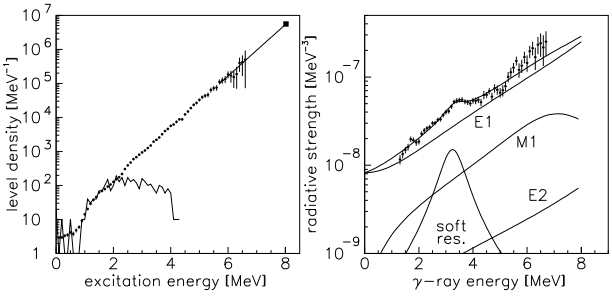

FIG. 1: Left panel: total level density of ^{172}Yb (filled circles), constant-temperature extrapolation (solid line), level density at S_n from average neutron-resonance spacing (filled square) [18], and level density from counting of discrete levels (jagged line) [19]. Right panel: total RSF of ^{172}Yb (filled circles), fit to the data, and decomposition into RSFs of different multipolarities (solid lines). Inclusion of the soft resonance in the fit decreases $\chi^2_{\rm red}$ from $\sim$ 5.1 to $\sim$ 1.3. Since this value is close to unity, inclusion of additional non-statistical structures cannot significantly improve the fit.

and parity J^π_m

$$I_{if}(E_1,E_2) = \sum_{XL,XL',J^\pi_m} \frac{\Gamma^{XL}_{im}(E_1)}{\Gamma_i}\rho(E_m,J^\pi_m)\frac{\Gamma^{XL'}_{mf}(E_2)}{\Gamma_m} + \sum_{XL,XL',J^\pi_{m'}} \frac{\Gamma^{XL}_{im'}(E_2)}{\Gamma_i}\rho(E_{m'},J^\pi_{m'})\frac{\Gamma^{XL'}_{m'f}(E_1)}{\Gamma_{m'}}. \quad (2)$$

The sums in Eq. (2) are restricted to give valid combinations of the level spins and parities and the transition multipolarities XL. Summing over all possibilities is necessary since neither the ordering of the two γ rays, nor the multipolarities of the transitions nor the spins and parities of the intermediate levels are known. The two transition energies are correlated by $E_1 + E_2 = E_i - E_f$, thus, TSC spectra can be expressed as one-dimensional spectra of one transition energy E_γ only. TSC spectra are symmetric around $E^{\rm sym}_\gamma = (E_i - E_f)/2$; integration over E_γ yields twice the total TSC intensity I_{if} if both γ rays are counted in the spectra. The knowledge of the parities π_i[1] and π_f ensures that I_{if} depends roughly speaking on the product of two RSFs around $E^{\rm sym}_\gamma$ [17], i.e., $f^2_{E1} + f^2_{M1}$ for $\pi_i = \pi_f$ and $2\,f_{E1}\,f_{M1}$ for $\pi_i \neq \pi_f$. I_{if} depends also on the level density. This usually prevents drawing firm conclusions from TSC experiments alone [16]. A combined analysis of Oslo-type and TSC experiments, however, enables one, with the help of the experimental level density, to establish firmly the sum and product, respectively, of all contributions to f_{M1} and f_{E1} at energies of the soft resonance, thus determining its multipolarity [17]. For this goal, the partial widths of

[1] One assumes that only neutron s-wave capture occurs.

Eq. (2) are expressed via Eq. (1) in terms of RSFs and level densities for a certain spin and parity. Eq. (1) actually gives only the average value of the Porter-Thomas distributed partial widths [20]. The total width Γ is the sum over all partial widths. The distribution of total widths becomes more and more peaked with increasing number of components [20]. The level density for a given spin and parity is calculated from the total level density by

$$\rho(E_x, J_x^\pi) = \rho(E_x)\,\frac{1}{2}\,\frac{2J_x+1}{2\,\sigma^2}\exp\left[-\frac{(J_x+1/2)^2}{2\,\sigma^2}\right], \quad (3)$$

where σ is the spin cut-off parameter, and we assume equal numbers of positive- and negative-parity levels. This assumption and Eq. (3) have been verified from the discrete level schemes of rare-earth nuclei [21]. Thus, all quantities for calculating TSC spectra are based on experimental data. Furthermore, using Oslo data for the level density and RSF in statistical-model calculations have yielded total γ-cascade spectra after neutron capture in excellent agreement with experiment (see Fig. 5 in Refs. [6, 22]).

B. Experiment

The combined analysis is applied to the nucleus ^{172}Yb which has been investigated by the ^{173}Yb(^{3}He,$\alpha\gamma$)^{172}Yb reaction in Oslo and by the ^{171}Yb$(n,\gamma\gamma)^{172}$Yb reaction at the Lujan Center of the Los Alamos Neutron Science Center (LANSCE). The Oslo data have been reported in [5, 6] and the Oslo method will be described in more detail in Sect. IV A. With the help of the Brink-Axel hypothesis [23, 24] the Oslo method provides us with a level density and a total RSF. The RSF can then be decomposed into a constant-temperature[2] KMF $E1$ model [4], a single-humped spin-flip $M1$ model, and a soft dipole resonance [6]. These models are chosen since they give a good phenomenological description of the experimental RSF. In the present work, we have improved on the normalization of the level density and the RSF and included an isoscalar Lorentzian $E2$ model [18] giving

$$f_\Sigma = K(f_{E1} + f_{M1}) + E_\gamma^2\, f_{E2} + f_{\rm soft}, \quad (4)$$

where K is a scaling factor of the order of one. Since quadrupole transitions populate levels within a broader spin interval than dipole transitions, Eq. (4) is of an approximative nature only. Given the weakness of quadrupole transitions and the level of experimental uncertainties, however, this approximation is believed to be sufficient. The improved data, the fit to the total RSF, and its decomposition into different multipolarities are given in Fig. 1. The parameters for the $E1$ RSF are taken from [6], those for the $M1$ and $E2$ RSFs from [18], where we use the f_{E1}/f_{M1} systematics at $\sim$ 7 MeV giving values in agreement with ARC work [27]. The fit parameters are: the constant temperature of the KMF model $T = 0.34(3)$ MeV, the normalization coefficient $K = 1.7(1)$, and the three parameters of the soft resonance $E = 3.3(1)$ MeV, $\Gamma = 1.2(3)$ MeV, and $\sigma = 0.49(5)$ mb.[3]

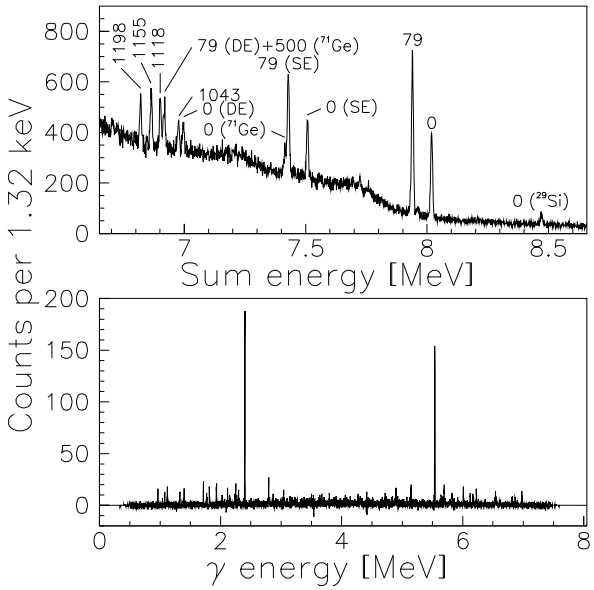

FIG. 2: Upper panel: energy-summed coincidence spectrum from the ^{171}Yb$(n,\gamma\gamma)^{172}$Yb reaction. Peaks are labeled by the energy of the final state. Peaks denoted by ^{71}Ge and ^{29}Si are due to n capture in the detector and in the glass ampoule, respectively. SE and DE stands for single- and double-escape peaks, respectively. Lower panel: TSC spectrum for the 2_1^+ final state. The slight asymmetry is due to the energy-dependent resolution of the detectors.

For the ^{171}Yb$(n,\gamma\gamma)^{172}$Yb experiment, we used $\sim$ 1 g of enriched, dry Yb_2O_3 powder encapsulated in a glass ampoule, mounted in an evacuated beam tube and irradiated by collimated neutrons with a time-averaged flux of $\sim 4\times10^4$ neutrons/cm^{2}s at $\sim$ 20 m from the thermal moderator. γ rays were detected by one shielded and segmented $\sim$ 200% clover and two 80% Ge(HP) detectors, placed at $\sim$ 12 cm from the target in a geometry

[2] The constant temperature compared to an excitation-energy dependent temperature in the KMF model is motivated by (i) the resemblance of the level density to a constant-temperature model, (ii) a better phenomenological descriptions of the total RSF, (iii) self consistency with the Brink-Axel hypothesis, and (iv) improved descriptions of isomeric- and photon-production cross sections in other rare-earth nuclei, see, e.g., [25, 26].

[3] The cited parameters are mean values obtained from the ^{173}Yb (^{3}He,$\alpha\gamma$)^{172}Yb and ^{172}Yb(^{3}He,^{3}He$'\gamma$)^{172}Yb reaction data reported in Ref. [28].

to minimize angular-correlation effects and contributions from higher-multiplicity cascades. Single and coincident γ rays were recorded simultaneously. The experiment ran for $\sim$ 150 h yielding $\sim 10^7$ coincidences. The relative detector efficiencies from 1–9 MeV were determined by two separate runs of $\sim$ 12 h each, before and after the ^{171}Yb$(n,\gamma\gamma)^{172}$Yb experiment, using the ^{35}Cl$(n,\gamma)^{36}$Cl reaction and its known γ intensities [29]. Also, a standard calibrated ^{60}Co source has been measured to adjust the relative curves to an absolute scale. The energy-summed coincidence spectrum (Fig. 2, upper panel) shows distinct peaks corresponding to TSCs between S_n and several low-lying states. The two strongest peaks have $\sim$ 4000 counts each. TSC spectra were obtained by gating on four peaks, one of them is displayed in the lower panel of Fig. 2. Relative intensities of primary versus secondary γ rays were determined from singles spectra and are in agreement with Ref. [27] but contradict the, in the literature, preferred data of Ref. [30] by a factor of three. Absolute primary intensities were determined by using new data on absolute secondary γ-ray intensities [31] and subsequent scaling of primary intensities to these values using the relative intensities of [27]. These absolute primary intensities are $\sim$ 20% higher than in [27]. TSC intensities are normalized to (i) the absolute primary intensity and secondary branching ratio of one, strong, individual TSC and (ii) by effectively estimating the number of neutron captures during the experiment from secondary singles lines, their absolute intensities, and absolute detector efficiencies. Both methods give equal results within their error bars.

C. Analysis and results

TSC intensities are compared to calculations according to Eq. (2) assuming either $E1$ or $M1$ multipolarity for the soft resonance [17]. One parameter in these calculations is the contribution to the thermal radiative neutron-capture cross section $\sigma^{\rm th}_{n,\gamma}$ from the two possible spins (0^- and 1^-) involved in neutron s-wave capture on ^{171}Yb. The compilation [32] assumes 0^- for the sub-threshold resonances which contribute 88% to $\sigma^{\rm th}_{n,\gamma}$. Another 4% comes from 0^- resonances above threshold, giving in total a 92% contribution of 0^- states. On the other hand, there is no strong evidence that all contributing sub-threshold resonances have 0^-. Examination of hard primary γ rays [27, 30] reveals many strong transitions populating 2^+ levels, indicating that a sizeable portion of $\sigma^{\rm th}_{n,\gamma}$ stems from 1^- resonances. Therefore, we performed calculations for a set of ratios $R = \sigma^{\rm th}_{n,\gamma}(0^-)/\sigma^{\rm th}_{n,\gamma}$. These calculations show, however, that only the TSC intensity to the 0^+_1 state has a strong dependence on this ratio.

In order to estimate the effect of Porter-Thomas fluctuations, we performed 100 Monte-Carlo simulations for each value of R assuming either $M1$ or $E1$ multipolarity of the soft resonance. In the simulations every partial radiative width is randomized according to the Porter-Thomas distribution. Total widths are calculated as a sum of randomized partial widths. To minimize the impact of Porter-Thomas fluctuations, we only compare TSC intensities integrated over a $\sim$2.4-MeV-broad energy range in the center of the spectra [16] (left panels of Fig. 3).

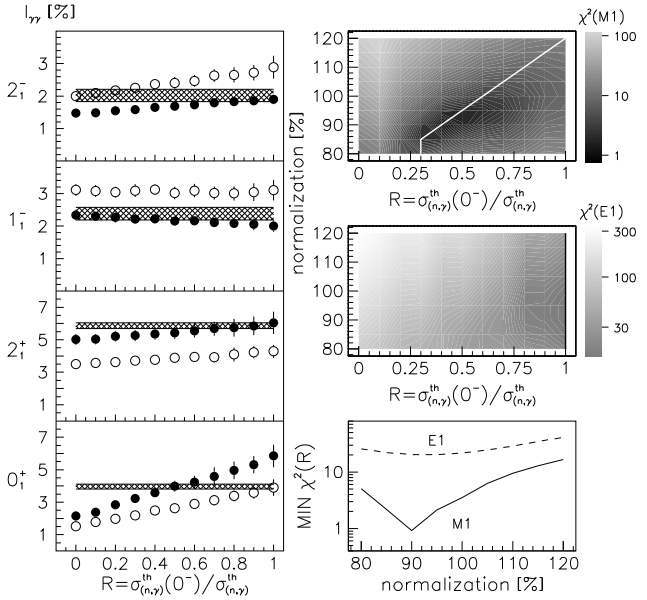

FIG. 3: Left: range of allowed experimental values (hatched areas) for TSC intensities to final states (from top to bottom) 2^-_1 at 1198 keV, 1^-_1 at 1155 keV, 2^+_1 at 79 keV, and the 0^+_1 ground state of ^{172}Yb. Full and open symbols correspond to calculations for different R with $M1$ and $E1$ multipolarity for the soft resonance, respectively. Error bars are estimated uncertainties due to Porter-Thomas fluctuations. Right: combined χ^2 for all four TSC intensities as function of R and N for $M1$ (upper panel) and $E1$ multipolarity (middle panel). The lines connect minimal values of χ^2 with respect to variations in R for any given N. For $E1$ multipolarity, this minimum is always obtained for $R = 1$ irrespective of N. Lower right: projection of the χ^2 surface onto the lines in the panels above.

Systematic errors not included in the statistical uncertainties are (i) corrections due to non-isotropic angular correlations of TSCs which have been estimated to be less than $\sim$ 3% and are thus neglected, (ii) uncertainties in the absolute scale of our detection efficiency, and (iii) uncertainties of primary and secondary intensities. The latter two uncertainties result in correlated uncertainties of the absolute scale of all four integrated TSC intensities in the order of $\sim$ 10–20%. Comparison between experiment and calculation is therefore performed for a number of overall normalization factors N applied to all four experimental TSC intensities simultaneously. χ^2 surfaces assuming $M1$ and $E1$ multipolarity of the soft resonance are calculated as function of R and N (upper right panels of Fig. 3). The least χ^2 of 20.2 for $E1$ multipolarity is obtained for $R = 1.0$ and $N = 95\%$. The least

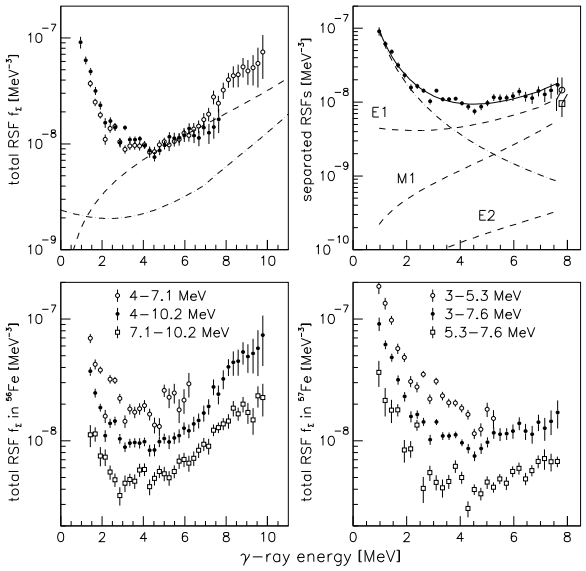

FIG. 4: Upper left: total RSF f_Σ of ^{57,56}Fe (filled and open circles, respectively), Lorentzian (dashed line) and KMF model (dash-dotted line) descriptions of the GEDR. Upper right: fit (solid line) to ^{57}Fe data and decomposition into the renormalized $E1$ KMF model, Lorentzian $M1$ and $E2$ models (all dashed lines), and a power law to model the large enhancement for low energies (dash-dotted line). Open symbols are estimates of the $E1$ (circle) and $M1$ (square) RSF from hard primary γ rays [11]. Lower panels: total RSF in ^{56}Fe (left) and ^{57}Fe (right) for different excitation-energy windows indicated in the figure. Open circles and squares are offset by a factor of 2 and 0.5 with respect to their true values.

χ^2 of 0.92 for $M1$ multipolarity is obtained for $R = 0.4$ and $N = 90\%$ (lower right panel of Fig. 3). Within our assumptions we can therefore rule out $E1$ multipolarity for the soft resonance on a high confidence level. More generally, the ability to describe all four integrated TSC intensities with one set of values for N, R, and the multipolarity of the soft resonance constitutes independent support for the experimental values of the level density and total RSF from the Oslo experiment and the validity of the decomposition of the latter. More pointedly, since the level density and total RSF (including its decomposition) have been published before the present TSC experiment had even been performed, the calculated TSC intensities are *de facto* predictions which are confirmed by the present experiment for one reasonable set of values for N, R, and the $M1$ hypothesis for the soft resonance.

D. Comparison with literature data

Since the multipolarity of the soft resonance has been established to be $M1$ by the TSC experiment, we can calculate its integrated strength as

$$B(M1\uparrow) = \frac{9\hbar c}{32\pi^2}\left(\frac{\sigma\Gamma}{E}\right)_{\rm soft} \qquad (5)$$

giving a value of 6.5(15) $\mu_{\rm N}^2$ which is entirely determined from the Oslo-type experiment. This is in agreement with the sum-rule approach for soft, orbital $M1$ strength assuming bare g factors[4] [33] but is more than twice the ground-state strength reported from NRF experiments [15]. This discrepancy has generated a great deal of controversy. A thorough discussion of this is far beyond the scope of this work and would in our opinion unduly shift the focus away from our experimental result which is the determination of the multipolarity of a previously observed, soft resonance in the RSF of ^{172}Yb. Thus, we will only make a few short comments. Firstly, detailed data on ground-state transitions from NRF experiments constrain very little the analysis of the present experiment. This is because only a very small fraction of the observed integrated TSC intensity can be attributed to transitions which have been previously observed in NRF experiments. Inspecting the experimental TSC spectra at γ energies for which strong ground-state transitions have been observed in NRF experiments shows that TSC intensities with these particular γ energies are in no way enhanced over TSC intensities with other γ energies. This is explained by the fact that TSC experiments are not sensitive to absolute ground-state decay widths, but only to branching ratios. Secondly, integrated TSC intensities are not sensitive to the degree of fragmentation or concentration of strength. This has implications for any direct comparison of NRF data with the present results. Thirdly, instead of the 4-MeV-wide $M1$ spin-flip resonance based on the work of Kopecky [34, 35] and adapted in [18] we have investigated an 8-MeV-wide $M1$ spin-flip model which simulates the two-humped $M1$ response observed in inelastic proton scattering off ^{154}Sm [36]. However, in order not to contradict the experimental f_{E1}/f_{M1} systematics at 7 MeV, such a model has to have twice the integrated strength than the 4-MeV-wide $M1$ spin-flip model by Kopecky. This gives rise to an increase of the χ^2 to 6.8 for a corresponding calculation as in Fig. 3 assuming $M1$ multipolarity for the soft resonance. For further discussions of the discrepancy between the present result and the results from NRF measurements we refer to Refs. [16, 37]. Also, a soft $M1$ resonance with similar strength as ours has been observed by another group [38], however, their analysis is based on schematic models for the level density and total RSF.[5]

[4] Bare g factors are likely appropriate for excitations built upon states above the pairing gap, i.e., in the quasicontinuum, which are the subject of the present work.

[5] One inconsistency in their analysis is the use of a variable temperature in the KMF model and a constant temperature in the level-density model

The discussion in their article provides some complementary comments on the discrepancy between their observation of an enhanced scissors-mode strength and the NRF results.

E. Summary of Sect. II

To conclude this first part, the soft resonance found in the decomposition of the total RSF of ^{172}Yb from Oslo-type experiments has been determined to be of $M1$ multipolarity by an auxiliary TSC measurement. The strength of the $M1$ resonance is $B(M1\uparrow) = 6.5(15)\ \mu_{\rm N}^2$ which is entirely determined by the former experiment. Assuming $M1$ multipolarity for similar soft resonances in other rare-earth nuclei investigated by the Oslo method gives consistent strengths of $\sim 6\ \mu_{\rm N}^2$ for various even and odd Dy, Er, and Yb nuclei, and reduced strengths of $\sim 3\ \mu_{\rm N}^2$ for the more spherical Sm nuclei; the centroids of these resonances increase weakly with mass number [22]. Our observation constitutes a virtually model-independent identification of the scissors mode in the quasicontinuum. The strength of this elementary $M1$ excitation in the quasicontinuum is twice the strength of the respective ground-state excitation. It is controversial whether this discrepancy is due to a genuine physics effect such as the response to a finite temperature, or whether there might be more mundane explanations related to deficiencies in the respective experiments or analysis methods. It will be interesting to see how this conflict is resolved in the future.

III. ENHANCEMENT OF THE SOFT RSF IN ^{56,57}Fe

Lighter nuclei like ^{56,57}Fe are interesting from a more fundamental point of view. Nowadays this mass region has become accessible for large-scale shell-model Monte-Carlo calculations [39]. Furthermore, ^{56}Fe is thought to be the seed nucleus for the astrophysical r process and it is the main component of steel, one of the most widespread construction materials. These two facts make the investigation of the level density and RSF of Fe important to reliably predict the response of ^{56}Fe nuclei to a radiation field of, e.g., neutrons or γ rays.

A. Results from Oslo-type experiments

Oslo-type experiments provide level densities and total RSFs for the two iron isotopes ^{56,57}Fe. Details of the Oslo method are given in Sect. IV A; more specifics concerning the Oslo experiments on the iron isotopes can be found in [40]. The RSFs from the Oslo experiment are brought to an absolute scale by normalizing them to the average total radiative width $\langle\Gamma_\gamma\rangle$ of neutron resonances [6]. The error of the absolute normalization is estimated to be $\sim 20\%$. For normalization, the assumption of equal amounts of positive and negative parity states at any energy below S_n is made. The violation of this assumption for low excitation energies introduces a systematic error to the absolute normalization in the order of $\sim 4\%$. In the case of ^{56}Fe, also the value of $\langle\Gamma_\gamma\rangle$ has to be estimated from systematics. However, branching ratios needed for the subsequent analysis of TSC measurements are independent of the absolute normalization of the total RSF and are consequently not affected by the above assumptions. The normalized RSFs in ^{56,57}Fe are displayed in Fig. 4. To ensure that the total RSFs do not depend on excitation energy, we have extracted them also from two distinct partitions (in excitation energy) of the primary-γ matrices. The striking feature of the RSFs is a large strength for soft transitions which has not been observed in the case of rare-earth nuclei, where we used the same analysis tools [6].

The soft transition strength constitutes a more than a factor of ten enhancement over common RSF models recommended in compilations [18]. To our knowledge, no other model can at present reproduce the shape of the total RSF either. A schematic temperature dependence of the RSF is taken into account in the KMF model. It is, however, insufficient to describe the data. Phenomenologically, the data are well described as a sum of a renormalized KMF model, Lorentzian descriptions of the GMDR and the isoscalar $E2$ resonance, and a power law modeling the large enhancement at low energies

$$f_\Sigma = K\,(f_{E1} + f_{M1} + \frac{A}{3\,\pi^2\,c^2\,\hbar^2}\,E_\gamma^{-B}) + E_\gamma^2\,f_{E2}. \quad (6)$$

The parameters for the RSF models are taken from systematics [18]. The fit parameters for ^{57}Fe are $K = 2.1(2)$, $A = 0.47(7)$ mb/MeV, and $B = 2.3(2)$ (E_γ in MeV). However, the good description of the enhancement by a power law should not prevent possible interpretations as a low-lying resonance or a temperature-related effect.

To ensure that the observed enhancement is not connected to peculiarities of the nuclear reaction or analysis method, a TSC measurements based on thermal neutron capture has been performed to confirm the findings. It has been shown that TSC intensities from ordered spectra can be used to investigate the soft RSF [17, 41]. The TSC technique for thermal neutron capture has been described in [16, 42]. It is based on multiplicity-two events populating low-lying levels. Here, we will only give a brief description of some details.

B. TSC experiment

The TSC experiment, i.e., the ^{56}Fe$(n,2\gamma)^{57}$Fe reaction, was performed at the dual-use cold-neutron beam facility of the Budapest Research Reactor (see [43, 44] and references therein). About 2 g of natural iron was irradiated with a thermal-equivalent flux of 3×10^7 cm^{-2}s^{-1} of cold neutrons for ~ 7 days. Single and coincident γ rays were

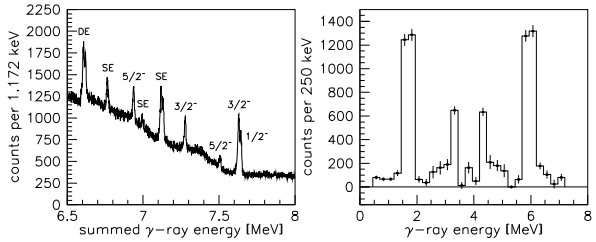

FIG. 5: Left panel: summed-energy spectrum for the ^{56}Fe $(n, 2\gamma)$ reaction. Peaks are labeled by the spin and parity of the final levels in ^{57}Fe. SE and DE denote single- and double-escape peaks. Right: efficiency-corrected and background-subtracted TSC spectrum gated on the unresolved doublet of the ground and first excited state. The spectrum is compressed into 250-keV-wide energy bins. Error bars include statistical errors only.

registered by two Ge(HP) detectors of 60% and 13% efficiency at a distance of 8 cm from the target and with an energy resolution of several keV. They were placed at 62.5° with respect to the beam axis in order to minimize the effect of angular correlations.

TSCs populating discrete low-lying levels in ^{57}Fe produce peaks in the summed-energy spectrum shown on the left panel of Fig. 5. Gating on the unresolved doublet of the $1/2^-$ ground state and the $3/2^-$ first excited state at 14 keV yields the TSC spectrum on the right panel of Fig. 5. Spectra to other final levels were not investigated due to their lower statistics and higher background. The TSC spectrum is compressed to 250-keV-wide energy bins. When the sequence of the two γ transitions is not determined experimentally, cascades with soft (discrete) secondary transitions are registered in the TSC spectrum as peaks on top of a continuum of cascades with soft primary transitions. Absolute normalization of TSC spectra is achieved by normalizing to five strong, discrete TSCs for which absolute intensities of their hard primary transitions and branching ratios for their secondary transitions are known [45]. The estimated error of the normalization is $\sim 20\%$. In the following, the smooth part of the TSC spectrum will be investigated in more detail.

In order to separate cascades with soft primary and soft secondary transitions in the TSC spectra, we use the fact that the spacing of soft, discrete secondary transitions in regions of sufficiently low level density is considerably larger compared to the detector resolution. Thus, soft secondary transitions will reveal themselves as discrete peaks. On the other hand, soft primary transitions will populate levels which are spaced much closer than the detector resolution and will hence create a continuous contribution. Separation of soft primary and secondary transitions is therefore reduced to a separation of individual peaks from a smooth continuum (by, e.g., a fitting procedure) in the appropriate energy interval [41].

The spin of the compound state in ^{57}Fe populated by s-wave neutron capture is $1/2^+$. Thus, in the excitation-energy region 0.55–1.9 MeV, there are only three levels which can be populated by primary $E1$ transitions: the $1/2^-$ level at 1266 keV, the $3/2^-$ level at 1627 keV, and the $3/2^-$ level at 1725 keV. All other levels have spins $5/2^-$ and higher and can only be populated by transitions with $M2/E3$ and higher multipolarity. Assuming that γ-transitions of such high multipolarities have a negligible contribution to the TSC spectrum, we do not take them into account in the further analysis. TSCs to the ground and first excited states involving the three above-mentioned levels as intermediate levels can easily be identified by the corresponding peaks in the TSC spectrum. Their contribution to the TSC spectra is subtracted. The remaining, continuous TSC spectrum in the specified energy range can be assigned to TSCs with soft primary-γ transitions. This smooth part of the TSC spectrum is used to test the soft RSF obtained from the Oslo-type experiment. Estimations based on the known level density in ^{57}Fe [40] show that soft primary transitions in the energy interval 0.55–1.9 MeV populate ~ 150 levels. Assuming that primary and secondary transitions fluctuate according to a Porter-Thomas distribution, we estimate systematic intensity uncertainties to be $\sim 25\%$ for this energy interval. Finally, also the mid point of the TSC spectrum, where energies of primary and secondary transitions are equal (and hence, known) has been used in the subsequent analysis. For other energy intervals, the determination of the sequence of the two transitions in TSCs is subject to large uncertainties, thus, they are unsuitable for the present analysis.

In the present analysis, the intensity of ordered[6] TSCs between an initial and final state is calculated on the basis of the statistical model of γ-decay from compound states

$$I_{if}(E_1, E_2) = \sum_{XL, XL', J^\pi_m} \frac{\Gamma^{XL}_{im}(E_1)}{\Gamma_i} \rho(E_m, J^\pi_m) \frac{\Gamma^{XL'}_{mf}(E_2)}{\Gamma_m}, \quad (7)$$

where E_1 and E_2 are the energies of the first and second transition in the TSC. More details on the TSC method are given in Sect. II A.

C. Analysis and results

Statistical-model calculations with experimental values for the level density and the total RSF have been performed assuming the decomposition of f_Σ according to Eq. (6), and a standard spin-parity distribution for in-

[6] Ordered TSC spectra are obtained by ensuring experimentally that the γ ray with energy E_1 is the first γ ray in the cascade and the γ ray with energy E_2 is the second one, such that Eq. (2) reduces to Eq. (7).

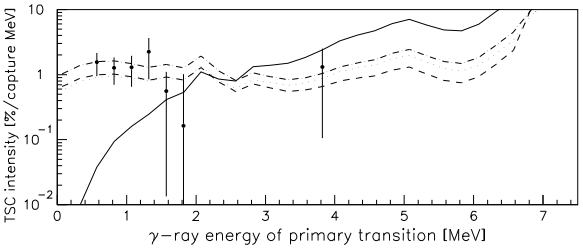

FIG. 6: Experimental TSC intensities in ^{57}Fe (compressed to 250-keV-broad γ energy bins) for cascades with soft primary γ rays and at the mid point of the spectrum (data points with error bars). Error bars include statistical and systematic uncertainties due to Porter-Thomas fluctuations. Lines are statistical-model calculations based on experimental data for the level density and f_Σ, neglecting (solid line) and assuming $E1$ (dashed line), $M1$ (dash-dotted line), and $E2$ (dotted line) multipolarity for the soft pole of the RSF.

termediate states [21]. Four calculations were performed: one by neglecting the third term in Eq. (6), i.e., without the soft pole of the RSF, the other three under the assumption of $E1$, $M1$, and $E2$ multipolarity, respectively, for this term. In Fig. 6, results are compared to experimental data for energies where ordering of TSCs can be achieved. The calculation without the soft pole does not reproduce the data at all. The experimental TSC intensity integrated over the 0.5–2.0-MeV energy region exceeds the calculated one by a factor of 4.8(1). For calculations under the assumption of $E1$, $M1$, and $E2$ multipolarities for the soft pole, this factor is reduced to 1.3(4), 1.0(3) and 1.4(4), respectively. Thus, any multipolarity is acceptable. Since the two lowest data points require an extrapolation of the total RSF below 1 MeV γ energy, we have performed calculations with different extrapolations including a resonance and an exponential description of the enhanced soft transition strength, avoiding the pole for $E_\gamma \rightarrow 0$. For these extrapolations the experimental TSC intensity for the lowest γ energy is not so well reproduced as before. Finally, we have performed calculations where the ratio of the negative-parity levels to the total number of levels decreases linearly from $\sim 90\%$ at 2.2 MeV to $\sim 50\%$ at ~ 7.6 MeV excitation energy. As expected, TSC intensities with soft primary γ rays are rather insensitive to this variation as well.

D. Summary of Sect. III

In conclusion, a more than a factor of 10 enhancement of soft transition strengths (a soft pole) in the total RSF has been observed in Oslo-type experiments using the ^{57}Fe(^{3}He,$\alpha\gamma$)^{56}Fe and ^{57}Fe(^{3}He,^{3}He$'\gamma$)^{57}Fe reactions. This enhancement cannot be explained by any present theoretical model. The total RSF has been decomposed into a KMF model for $E1$ radiation, Lorentzian models for $M1$ and $E2$ radiation, and a power law to model the soft pole. In a second experiment, TSC intensities from the ^{56}Fe$(n,2\gamma)^{57}$Fe reaction were measured. Statistical-model calculations based on RSFs and level densities from the Oslo-type experiment were performed. These calculations can reproduce the experimental TSC intensities with soft primary γ rays only in the presence of the soft pole in the total RSF. The uncertainties due to Porter-Thomas fluctuations of TSC intensities do not allow us to draw definite conclusions about the multipolarity of the soft pole. For better selectivity, averaging over many initial n resonances will be needed. The satisfying reproduction of the experimental TSC data constitutes support for the physical reality of the soft pole, independent from the Oslo-type experiment. It should be noted that this support was gained by using a different nuclear reaction, a different type of detector, and a different analysis method. Finally, as further supporting evidence, we would like to mention that preliminary results on a chain of stable Mo isotopes also indicate the presence of a soft pole in the total RSF (see Sect. IV and [46]), while in the case of ^{27,28}Si, the Oslo method was able to reproduce the total RSF constructed from literature data on energies, lifetimes, and branching ratios available for the complete level schemes [47].

IV. ENHANCEMENT OF THE SOFT RSF IN A CHAIN OF Mo ISOTOPES

The stable molybdenum isotopes are well suited as targets for the study of nuclear properties when going from spherical to deformed shapes. In this Section we discuss a systematic analysis of the RSFs of the six $^{93-98}$Mo isotopes. The RSFs depend on the dynamic properties of electric charges present within these systems ($Z = 42$). Since the nuclear deformation varies from spherical shapes ($\beta \sim 0$) at $N = 51$ to deformed shapes ($\beta \sim 0.2$) at $N = 56$, we expect to observe effects due to shape changes. Furthermore, these nuclei reveal weak GEDR tails at low E_γ, making them interesting objects in the search for other weak structures in the RSF.

A. Oslo-type experiment

The particle-γ coincidence experiments were carried out at the OCL for $^{93-98}$Mo using the CACTUS multidetector array. The charged ejectiles were detected by eight Si particle telescopes placed at an angle of 45° relative to the beam direction. Depending on target-thickness and the size of the collimators in front of the Si telescopes, the kinematically dominated energy resolution can be up to ~ 250 keV. An array of 28 NaI $5'' \times 5''$ γ-ray detectors with a total efficiency of $\sim$15% of 4π and an energy resolution of $\sim 6\%$ at 1.3 MeV surrounded the

target and particle detectors.

In this Section, results from eight different reactions on four different targets are discussed. Typical experiments were run with 45-MeV beam energy. However, for some Mo isotopes, we have chosen a somewhat smaller beam energy of 30 MeV. The beam energies for the different reactions are given in parentheses.
1) ^{94}Mo(^{3}He,$\alpha\gamma$)^{93}Mo (30 MeV)
2) ^{94}Mo(^{3}He,^{3}He$'\gamma$)^{94}Mo (30 MeV)
3) ^{96}Mo(^{3}He,$\alpha\gamma$)^{95}Mo (30 MeV)
4) ^{96}Mo(^{3}He,^{3}He$'\gamma$)^{96}Mo (30 MeV)
5) ^{97}Mo(^{3}He,$\alpha\gamma$)^{96}Mo (45 MeV)
6) ^{97}Mo(^{3}He,^{3}He$'\gamma$)^{97}Mo (45 MeV)
7) ^{98}Mo(^{3}He,$\alpha\gamma$)^{97}Mo (45 MeV)
8) ^{98}Mo(^{3}He,^{3}He$'\gamma$)^{98}Mo (45 MeV)
The targets were self-supporting metal foils typically enriched to $\sim 95\%$ with thicknesses of ~ 2 mg/cm^2. The experiments were run with beam currents of ~ 2 nA for 1–2 weeks. The reaction spin windows are typically $I \sim 2-6\hbar$.

The experimental extraction procedure and the assumptions made are described in Refs. [5, 48] and references therein. For each initial excitation energy E_i, determined from the ejectile energy and reaction Q value, γ-ray spectra are recorded. Then the spectra are unfolded using the known γ-ray response function of the CACTUS array [49]. These unfolded spectra are the basis for making the first-generation (or primary) γ-ray matrix [50], which is factorized according to the Brink-Axel hypothesis [23, 24], by

$$P(E, E_\gamma) \propto \rho(E - E_\gamma)\, f_\Sigma(E_\gamma)\, E_\gamma^3. \quad (8)$$

The level density and total RSF can be determined by an iterative procedure [5] through the adjustment of each data point of these two functions until a global χ^2 minimum of the fit to the experimental $P(E_i, E_\gamma)$ matrix is reached. It has been shown [5] that if one solution for the multiplicative functions ρ and f_Σ is known, one may construct an infinite number of other functions, which give identical fits to the P matrix by

$$\tilde{\rho}(E_i - E_\gamma) = \mathcal{A} \exp[\alpha(E_i - E_\gamma)]\, \rho(E_i - E_\gamma), \quad (9)$$

$$\tilde{f}_\Sigma(E_\gamma) = \mathcal{B} \exp(\alpha E_\gamma) f_\Sigma(E_\gamma). \quad (10)$$

Consequently, neither the slope (α) nor the absolute values of the two functions ($\mathcal{A}$ and $\mathcal{B}$) can be obtained through the fitting procedure.

The parameters $\mathcal{A}$ and α can be determined by normalizing the level density to the number of known discrete levels at low excitation energy [45] and to the level density estimated from neutron-resonance spacing data at the neutron binding energy S_n [18]. The procedure for extracting the total level density ρ from the resonance energy spacing D is described in Ref. [5]. Here, we will discuss only the determination of parameter $\mathcal{B}$ of Eq. (10), which gives the absolute normalization of f_Σ. For this purpose we utilize experimental data on the average total radiative width $\langle\Gamma_\gamma\rangle$ of neutron resonances at S_n.

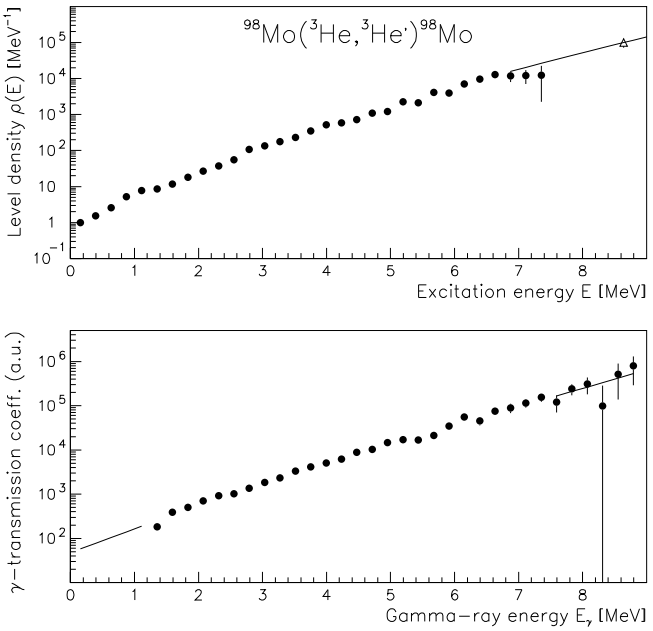

FIG. 7: Measured level density ρ (upper panel) and radiative transmission coefficient $2\pi\, E_\gamma^3\, f_\Sigma$ (lower panel) for ^{98}Mo. The straight lines are extrapolations needed to calculate the normalization integral of Eq. (11). The triangle in the upper panel is based on resonance spacing data at S_n.

We assume here that the γ decay in the continuum is dominated by $E1$ and $M1$ transitions. For initial spin I and parity π at S_n, the width can be written in terms of the RSF by [51]

$$\langle\Gamma_\gamma\rangle = \frac{1}{2\rho(S_n, I, \pi)} \sum_{I_f} \int_0^{S_n} \mathrm{d}E_\gamma\, \mathcal{B}\, E_\gamma^3\, f_\Sigma(E_\gamma)\, \rho(S_n - E_\gamma, I_f), \quad (11)$$

where the summation and integration run over all final levels with spin I_f, which are accessible by γ radiation with energy E_γ and multipolarity $E1$ or $M1$.

A few considerations have to be made before $\mathcal{B}$ can be determined. Methodical difficulties in the primary γ-ray extraction prevents determination of the functions $f_\Sigma(E_\gamma)$ in the interval $E_\gamma < 1$ MeV and $\rho(E)$ in the interval $E > S_n - 1$ MeV. In addition, $f_\Sigma(E_\gamma)$ at the highest γ energies, above $E_\gamma \sim S_n - 1$ MeV, suffers from poor statistics. For the extrapolation of ρ we apply the back-shifted Fermi-gas level density as demonstrated in Ref. [21]. For the extrapolations of $E_\gamma^3\, f_\Sigma$ we use an exponential form. As a typical example, the extrapolations for ^{98}Mo are shown in Fig. 7. The contribution of the extrapolations of ρ and f_Σ to the calculated radiative width in Eq. (11) does not exceed 15% [6]. The experimental widths $\langle\Gamma_\gamma\rangle$ in Eq. (11) are listed in Table I. For ^{94}Mo, this width is unknown and is estimated by an extrapolation based on the ^{96}Mo and ^{98}Mo values.

TABLE I: Parameters used for the RSFs. The data are taken from Ref. [18]. The $E1$ resonance parameters for the even Mo isotopes are based on photo absorption experiments [2] and the parameters for the odd Mo isotopes are derived from interpolations.

Nucleus	E_{E1} (MeV)	σ_{E1} (mb)	Γ_{E1} (MeV)	E_{M1} (MeV)	σ_{M1} (mb)	Γ_{M1} (MeV)	E_{E2} (MeV)	σ_{E2} (mb)	Γ_{E2} (MeV)	$\langle\Gamma_\gamma\rangle$ (meV)
^{93}Mo	16.59	173.5	4.82	9.05	0.86	4.0	13.91	2.26	4.99	160(20)
^{94}Mo	16.36	185.0	5.50	9.02	1.26	4.0	13.86	2.24	4.98	170(40) [a]
^{95}Mo	16.28	185.0	5.76	8.99	1.38	4.0	13.81	2.22	4.97	135(20)
^{96}Mo	16.20	185.0	6.01	8.95	1.51	4.0	13.76	2.21	4.96	150(20)
^{97}Mo	16.00	187.0	5.98	8.92	1.58	4.0	13.71	2.19	4.95	110(15)
^{98}Mo	15.80	189.0	5.94	8.89	1.65	4.0	13.66	2.17	4.93	130(20)

[a]Estimated from systematics

The RSFs extracted from the eight reactions are displayed in Fig. 8. As expected, the RSFs seem not to show any odd-even mass differences. The results obtained for the (^{3}He,α) and (^{3}He,^{3}He$'$) reactions populating the same residual nucleus reveal very similar RSFs. Also for ^{96}Mo two different beam energies have been applied, giving very similar RSFs. Thus, the observed energy and reaction independence gives further confidence in the Oslo method.

B. Description of the RSFs

An inspection of the experimental RSFs of Fig. 8 reveals that the RSFs are increasing functions of γ energy for $E_\gamma > 3$ MeV. This indicates that the RSFs are influenced by the tails of the giant resonances. As follows from previous work, the main contribution (about 80%) is due to the GEDR. The GMDR and the isoscalar $E2$ resonance are also present in this region.

If the GEDR is described by a Lorentzian function, one will find that the strength function approaches zero in the limit of $E_\gamma \to 0$. However, the ^{144}Nd(n,$\gamma\alpha$) reaction [3] strongly suggests that f_{E1} has a finite value in this limit. The KMF model [4] describes this feature for the electric dipole RSF:

$$f_{E1}(E_\gamma, T) = \frac{1}{3\pi^2\hbar^2c^2}\frac{0.7\sigma_{E1}\Gamma_{E1}^2(E_\gamma^2+4\pi^2T^2)}{E_{E1}(E_\gamma^2-E_{E1}^2)^2}. \quad (12)$$

The temperature T depends on the final state f and for simplicity we adapt the schematic form

$$T(E_f) = \sqrt{U_f/a}, \quad (13)$$

where the level density parameter is parameterized as $a = 0.21A^{0.87}$ MeV^{-1}. The intrinsic energy is estimated by $U_f = E_f - C_1 - E_{\rm pair}$ with a back-shift parameter of $C_1 = -6.6A^{-0.32}$ MeV [52]. The pairing energy contribution $E_{\rm pair}$ is evaluated from the three-point mass formula of Ref. [53].

Although the KMF model has been developed for spherical nuclei, it has been successfully applied to ^{56,57}Fe (see Sect. III) and several rare-earth nuclei (see Sect. II and Refs. [6, 10, 21, 22]) assuming a constant-temperature parameter T in Eq. (12), i.e., one that is independent of excitation energy. In this work we assume that the temperature depends on excitation energy according to Eq. (13) which gives an increase in the RSF at low γ energy [21].

In order to compare the excitation-energy dependent RSF with experiments, Eq. (12) should be folded with the final excitation energies of the specific experiment giving

$$\langle f_{E1}(E_\gamma)\rangle = \frac{1}{E_2-E_1}\int_{E_1-E_\gamma}^{E_2-E_\gamma} {\rm d}E_f f_{E1}(E_f), \quad (14)$$

where the integration runs over all final excitation energies E_f which are experimentally accessible by transitions with given energy E_γ. Our dataset of primary γ-ray spectra is typically taken between $E_1 \sim 4$ MeV and $E_2 \sim S_n$ initial excitation energy.

The GMDR contribution to the total RSF is described by a Lorentzian

$$f_{M1}(E_\gamma) = \frac{1}{3\pi^2\hbar^2c^2}\frac{\sigma_{M1}E_\gamma\Gamma_{M1}^2}{(E_\gamma^2-E_{M1}^2)^2+E_\gamma^2\Gamma_{M1}^2}. \quad (15)$$

This approach is in accordance with numerous experimental data obtained so far, and is recommended in Ref. [18]. However, the experimental data scatter and the resonance parameter values are uncertain. This is also true for the $E2$ resonance. Although of minor importance, the $E2$ radiative strength f_{E2} has also been included. Here, we use the same Lorentzian function as in Eq. (15), but with different resonance parameters and an additional factor $3/(5E_\gamma^2)$. The resonance parameters for the $E1$, $M1$, and $E2$ resonances are taken from the compilation of Refs. [2, 18] and are listed in Table I.

The enhanced RSF at low γ energies has at present no theoretical explanation. Previously, a pygmy resonance

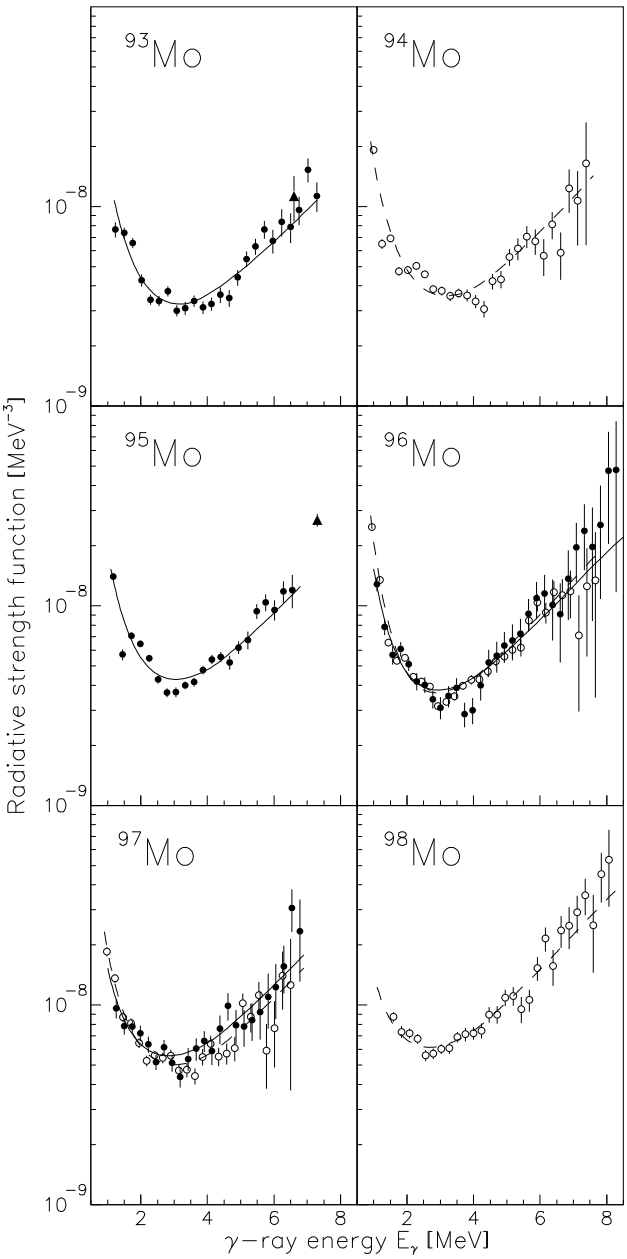

FIG. 8: Normalized RSFs for $^{93-98}$Mo. The filled and open circles represent data taken with the (^{3}He,α) and (^{3}He,^{3}He$'$) reactions, respectively. The filled triangles in ^{93,95}Mo are estimates of $E1$ RSFs using hard primary γ rays [11]. The solid and dashed lines are fits to the RSF data from the two respective reactions (see text).

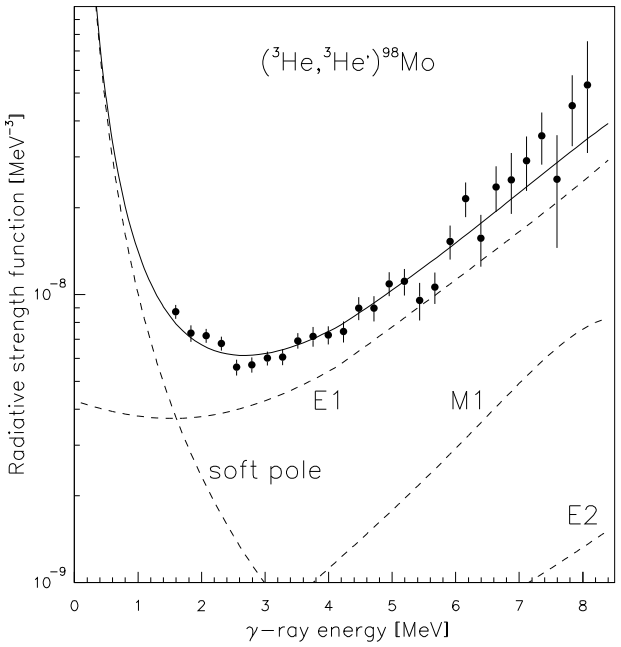

FIG. 9: Experimental RSF of ^{98}Mo compared to a model description including GEDR, GMDR, and the isoscalar E2 resonance. The empirical soft-pole component is used to describe the low-energy part of the RSF.

around $E_\gamma \sim 3$ MeV has been reported in several rare-earth nuclei [6, 21, 22]. The electromagnetic character of the corresponding RSF structure is now established to be of $M1$ type [7, 38] and is interpreted as the scissors mode (see Sect. II). Deformed nuclei can in principle possess this collective motion, and, e.g., ^{98}Mo with a deformation of $\beta \sim 0.18$ could eventually show some reminiscence of the scissors mode. Data on ^{94}Mo [54] and ^{96}Mo [55] show a summed $M1$ strength to mixed symmetry 1^+ states around ~ 3.2 MeV in the order of $\sim 0.6\mu_N^2$. This is about one order of magnitude lower than the $M1$ strength observed in well-deformed rare-earth nuclei using the present method. This $M1$ strength is deemed too weak to cause a visible bump in our RSFs above 3 MeV.

Recently, a similar enhancement as in the Mo isotopes has been observed for the soft RSF in iron isotopes [8, 10] (see Sect. III). We called this structure a soft pole in the RSF and chose a simple power law parameterization given by Eq. (6) which we think is also a reasonable decomposition of the total RSF of Mo isotopes.

Within this description of the total RSF there are three fit parameters: K, A, and B. The factor K is an overall scale parameter. Generally, its value deviates from unity for several reasons; the most important reasons are theoretical uncertainties in the KMF model and the evaluation of $\mathcal{B}$ in Eq. (11). The values of the fit parameters for the eight reactions are summarized in Table II.

In Fig. 9 the various contributions to the total RSF of ^{98}Mo are shown. The main components are the GEDR resonance and the unknown low-energy structure. We observe that the $E1$ component exhibits an increased yield for the lowest γ energies due to the increase in temperature T. However, this effect alone is not strong enough to explain the low-energy enhancement of the the total RSF.

Figure 8 shows the fit functions for all reactions and gives qualitative good agreements with the experimental data. The fitting parameters K, A and B are all similar within the uncertainties. It should be noted

TABLE II: Soft-pole fitting parameters and integrated strengths. The reduced $B(XL\uparrow)$ values are only lower estimates (see text).

Reaction	A (mb/MeV)	B	K	$B(E1\uparrow)$ (e^2fm^2)	$B(M1\uparrow)$ (μ_N^2)	$B(E2\uparrow)$ ($10^3\,e^2$fm^4)
(^{3}He,α)^{93}Mo	0.37(7)	2.6(3)	0.44(4)	0.021(5)	1.9(4)	14(3)
(^{3}He,^{3}He$'$)^{94}Mo	0.48(5)	2.5(2)	0.36(2)	0.023(3)	2.1(3)	16(2)
(^{3}He,α)^{95}Mo	0.48(6)	2.6(2)	0.39(2)	0.024(4)	2.2(3)	16(2)
(^{3}He,^{3}He$'$)^{96}Mo	0.60(4)	3.2(2)	0.36(1)	0.022(2)	2.0(2)	16(1)
(^{3}He,α)^{96}Mo	0.47(14)	2.7(6)	0.32(4)	0.019(7)	1.7(6)	13(4)
(^{3}He,^{3}He$'$)^{97}Mo	0.47(7)	2.4(3)	0.38(3)	0.025(5)	2.3(4)	16(3)
(^{3}He,α)^{97}Mo	0.30(10)	2.2(5)	0.45(5)	0.020(8)	1.9(7)	13(5)
(^{3}He,^{3}He$'$)^{98}Mo	0.22(7)	2.1(5)	0.52(4)	0.018(7)	1.6(6)	12(4)

that the soft-pole parameters coincide with the description of the soft pole in the ^{57}Fe nucleus [10] yielding $A = 0.47(7)$ mb/MeV and $B = 2.3(2)$.

The RSFs for $E_\gamma > 3$ MeV when going from $N = 51$ to 56 increase by almost a factor of 2 and this can be understood from the corresponding evolution of nuclear deformation. Following the onset of prolate deformation the GEDR will split into two parts, where 1/3 of its strength is shifted down in energy and 2/3 is shifted up. Photoneutron cross sections [2] do not show a splitting into two separate bumps, however, the observed increase in width Γ_{E1} as function of neutron number (see Table I) supports the idea of a splitting, which is a well-known feature in other more deformed nuclei. Figure 8 demonstrates that the adopted widths describe very well the variation of the RSF as function of mass number.

To investigate whether the prominent soft-pole structure is present in the whole excitation-energy region, we have performed the following test. Assuming that the level density from Eq. (8) is correct, we can estimate the shape of the strength functions starting at various initial excitation energies using

$$f(E_\gamma, E_i) = \frac{1}{2\pi}\frac{\mathcal{N}(E_i)P(E_i, E_\gamma)}{\rho(E_i - E_\gamma)E_\gamma^3}. \qquad (16)$$

Actually, $f(E_\gamma, E_f)$ would have been the proper expression to investigate, but due to technical reasons we choose $f(E_\gamma, E_i)$, which is equivalent to investigating $f(E_\gamma, E_f)$ because in our method E_f and E_i are uniquely related by $E_f = E_i - E_\gamma$. One problem is that the normalization constant is only roughly known through the estimate

$$\mathcal{N}(E_i) = \frac{\int_0^{E_i} \mathrm{d}E_\gamma\, \rho(E_i - E_\gamma)\, 2\pi\, f_\Sigma(E_\gamma)\, E_\gamma^3}{\int_0^{E_i} \mathrm{d}E_\gamma\, P(E_i, E_\gamma)} \qquad (17)$$

with $E_i < S_n$. However, for the expression $f(E_\gamma, E_i)$ we are only interested in the shape of the RSFs, and an exact normalization is therefore not crucial. The evaluation assumes that an eventual temperature-dependent behavior of the RSF is small compared to the soft-pole structure[7].

In Fig. 10, the RSFs for ^{96,98}Mo are shown at various initial energies E_i. For comparison, the figure also includes the global RSFs (solid lines) obtained with the Oslo method (Fig. 8). Within the error bars the data support that the soft pole is present for all the excitation-energy bins studied.

The origin of the soft pole cannot be explained by any known theoretical model. One would therefore need to know the γ-ray multipolarity as guidance for theoretical approaches to this phenomenon. Rough estimates of the reduced strength can be obtained from

$$B(XL\uparrow) = \frac{1}{8\pi}\frac{L\,(2L+1)\,[(2L+1)!!]^2}{L+1}(\hbar c)^{2L+1} \times \int_{1\mathrm{MeV}}^{3\mathrm{MeV}} \mathrm{d}E_\gamma f_{XL}(E_\gamma). \qquad (18)$$

In the evaluation, we have integrated the soft pole between 1 and 3 MeV. Thus, the estimates listed in Table II for the reactions studied give only a lower limit for the respective $B(XL\uparrow)$ values. The correct result will of course depend on the functional form of the soft pole below 1 MeV; however, no experimental data exist in this region and any assumption here would be highly speculative. There seems to be no clear dependency of the $B(XL\uparrow)$ values on mass number or nuclear deformation.

With the assumptions above, we get in the case of an $E1$ soft pole an average $B(E1\uparrow)$ value of 0.02 e^2fm^2, which is 0.07% of the sum rule for the GEDR. Assuming an $M1$ soft pole, we get roughly $B(M1\uparrow) \sim 2.0\ \mu_N^2$, which is 3–4 times larger than the observed strength to mixed symmetry 1^+ states around 3 MeV in ^{94}Mo [54] and ^{96}Mo [55].[8] Provided the soft pole has $E2$ multipolarity we obtain finally a $B(E2\uparrow)$ value around

[7] Simulations using the KMF model indicate a maximum 20% effect from a temperature dependence of the RSF.

[8] Interestingly, Ref. [54] also quotes a strong $M1$ transition with an energy of 721 keV from the 4_2^+ to the 4_1^+ state in ^{94}Mo with $B(M1\downarrow) = 1.23(20)\ \mu_N^2$ and a large transition-matrix el-

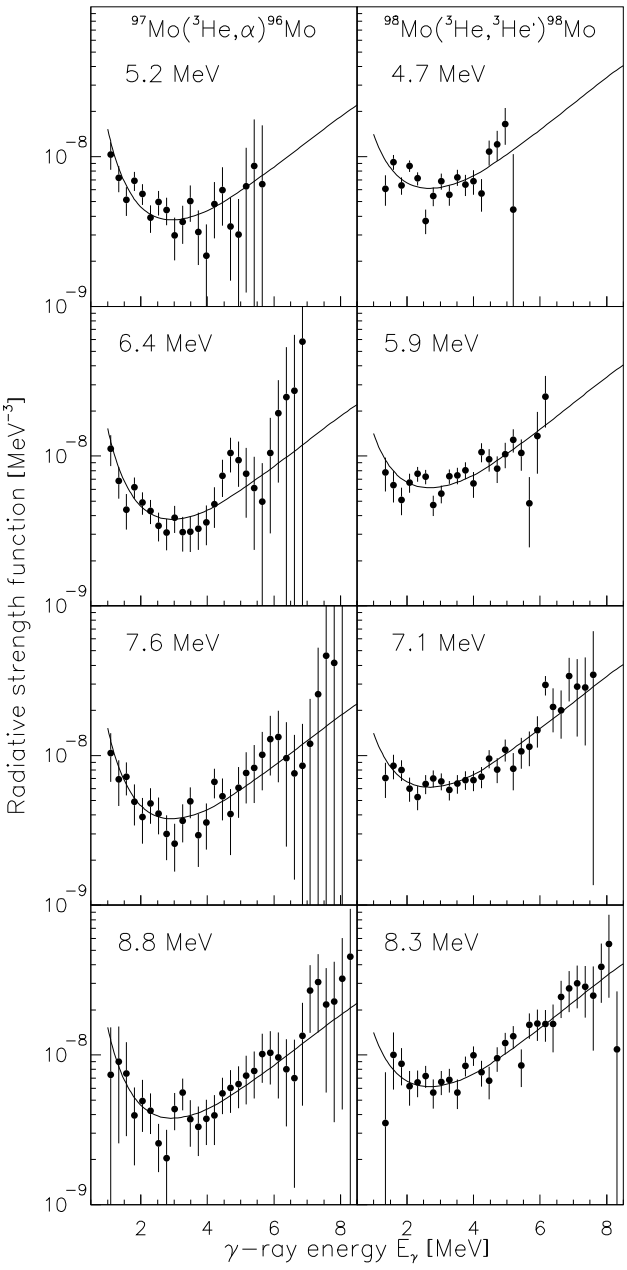

FIG. 10: RSFs for ^{96,98}Mo at various initial excitation energies. The soft pole is present for all E_i. The solid lines display the RSFs obtained in Fig. 8.

15000 e^2fm^4, which is 5–15 times larger than the ones for the excitation to the first excited 2^+ states in the even molybdenum isotopes. Thus, we cannot exclude any of these multipolarities, since neither of them would yield unreasonably high transition strengths. Moreover, we would like to point out that the observed soft pole resides on top of the tails of giant resonances. Thus, the transition strength included in the soft pole has to be added to the strength in the giant resonance tail of the correct multipolarity to give the summed transition strength.

ement $|\langle 4_1^+||M1||4_3^+\rangle|$ for a 991-keV transition in the order of 1.44(22) μ_N which indicates rather strong $M1$ excitations built on the excited 4_1^+ state. If such low-energy $M1$ strength is common for excitations in the quasicontinuum, it would make $M1$ multipolarity a good candidate for the soft pole observed in the present work.

C. Summary of Sect. IV

As expected, the observed RSFs reveal very similar shapes since they all refer to isotopes with the same nuclear charge. When going from $N = 51$ to 56 the RSFs increase by almost a factor of two for $E_\gamma > 3$ MeV, which can be understood from the change of nuclear deformation. With the onset of deformation, the increasing GEDR width Γ_{E1} is responsible for the increasing strength.

An enhanced strength at low γ energies is observed, which is equally strong for all isotopes and excitation energies studied. A similar enhancement has also been seen in the iron isotopes. The multipolarity of the soft-pole radiation is unknown and there is still no theoretical explanation for this very interesting phenomenon.

V. SUMMARY

In this work, we have investigated the soft RSF for transitions between warm states of several nuclei using two types of experiments, (i) Oslo-type experiments and (ii) TSC experiments. In the case of ^{172}Yb, the Oslo-type experiments yielded a strong resonance at 3 MeV γ energy. With an auxiliary TSC experiment, the multipolarity of this resonance could be determined as $M1$. The strength of this $M1$ resonance could then be determined as $B(M1\uparrow) = 6.5(15)\ \mu_N^2$ which is about twice the strength observed in NRF experiments. In the case of ^{57}Fe, the Oslo-type experiment yielded a strong (more than a factor of 10) enhancement of the soft RSF over common theoretical estimates. An auxiliary TSC experiment confirmed this observation but it was not possible to pin down the multipolarity of this strength. In the case of a chain of stable Mo isotopes, the Oslo-type experiments yielded a moderate (factor 3) enhancement of the soft RSF below 3 MeV γ energy. This enhancement has not yet been confirmed by TSC experiments.

In conclusion, we have shown that the combination of the Oslo method and TSC experiments is able to provide unique data on the soft RSF for transitions between warm states (several MeV above the yrast line). These unique data have already yielded stunning results which, in the case of rare-earth nuclei provide evidence of an enhanced scissors mode in the quasicontinuum and in the case of the lighter Fe and Mo isotopes provide first evidence for a completely unexpected enhancement of the

soft RSF beyond any present theoretical model. It is obvious that these kinds of investigations are very fruitful from a nuclear structure point of view. As possible applications of our data we would like to point out that the enhancement of the soft RSF might strongly alter model calculations for isomeric production cross sections in astrophysical environments or scenarios important for nuclear stockpile stewardship. This is especially true if a high γ multiplicity is needed to populate isomers with a spin far different from the average spin in the respective compound system. Also calculations of γ-production cross sections and average γ multiplicities will be affected by our data.

Acknowledgments

This work has benefited from the use of the Los Alamos Neutron Science Center at the Los Alamos National Laboratory. This facility is funded by the U.S. Department of Energy under Contract W-7405-ENG-36. Part of this work was performed under the auspices of the U.S. Department of Energy by the University of California, Lawrence Livermore National Laboratory under Contract W-7405-ENG-48 and Los Alamos National Laboratory under Contract W-7405-ENG-36. Financial support from the Norwegian Research Council (NFR) is gratefully acknowledged. Part of this work was supported by the EU5 Framework Programme under Contract HPRI-CT-1999-00099. G.E.M. and E.A. acknowledge support by U.S. Department of Energy Grant No. DE-FG02-97-ER41042. G.E.M., U.A., E.A., and A.V. acknowledge support from the National Nuclear Security Administration under the Stewardship Science Academic Alliances program through the U.S. Department of Energy Research Grant Nos. DE-FG03-03-NA00074 and DE-FG03-03-NA00076. A.V. acknowledges support from a NATO Science Fellowship under project number 150027/432. A.S. acknowledges support by the National Science Foundation Grant No. PHY01-10253. We thank Gail F. Eaton and Timothy P. Rose for making the targets.

[1] G. A. Bartholomew, E. D. Earle, A. J. Ferguson, J. W. Knowles, and M. A. Lone, Adv. Nucl. Phys. **7**, 229 (1973).
[2] Samuel S. Dietrich and Barry B. Berman, At. Data Nucl. Data Tables **38**, 199 (1988).
[3] Yu. P. Popov, in *Neutron Induced Reactions*, Proceedings of the Europhysics Topical Conference, Smolenice, 1982, edited by P. Oblozinský (Institute of Physics, Bratislava, 1982), p. 121.
[4] S. G. Kadmenskiĭ, V. P. Markushev, and V. I. Furman, Yad. Fiz. **37**, 277 (1983).
[5] A. Schiller *et al.*, Nucl. Instrum. Methods Phys. Res. A **447**, 498 (2000).
[6] A. Voinov *et al.*, Phys. Rev. C **63**, 044313 (2001).
[7] A. Schiller *et al.*, nucl-ex/0401038.
[8] E. Tavukcu, Ph.D. thesis, North Carolina University, 2002.
[9] M. Guttormsen *et al.*, Phys. Rev. C **71**, 044307 (2005).
[10] A. Voinov *et al.*, Phys. Rev. Lett. **93**, 142504 (2004).
[11] J. Kopecky and M. Uhl, in Proceedings of a Specialists' Meeting on Measurement, Calculation and Evaluation of Photon Production Data, Bologna, Italy, 1994, Report No. NEA/NSC/DOC(95)1, p. 119.
[12] S. Joly, D. M. Drake, and L. Nilsson, Phys. Rev. C **20**, 2072 (1979).
[13] M. Guttormsen, J. Rekstad, A. Henriquez, F. Ingebretsen, and T. F. Thorsteinsen, Phys. Rev. Lett. **52**, 102 (1984).
[14] M. Igashira, H. Kitazawa, M. Shimizu, H. Komano, and N. Yamamuro, Nucl. Phys. **A457**, 301 (1986).
[15] A. Zilges *et al.*, Nucl. Phys. **A507**, 399 (1990); **A519**, 848 (1990).
[16] F. Bečvář *et al.*, Phys. Rev. C **52**, 1278 (1995).
[17] A. Voinov *et al.*, Nucl. Instrum. Methods Phys. Res. A **497**, 350 (2003).
[18] *Handbook for Calculations of Nuclear Reaction Data* (IAEA, Vienna, 1998).
[19] R. Firestone and V. S. Shirley, *Table of Isotopes*, 8th ed. (Wiley, New York, 1996).
[20] C. E. Porter and R. G. Thomas, Phys. Rev. **104**, 483 (1956).
[21] M. Guttormsen *et al.*, Phys. Rev. C **68**, 064306 (2003).
[22] S. Siem *et al.*, Phys. Rev. C **65**, 044318 (2002).
[23] D. M. Brink, Ph.D. thesis, Oxford University, 1955.
[24] P. Axel, Phys. Rev. **126**, 671 (1962).
[25] O. T. Grudzevich, Yad. Fiz. **62**, 192 (1999).
[26] O. T. Grudzevich, Yad. Fiz. **63**, 484 (2000).
[27] R. C. Greenwood, C. W. Reich, and S. H. Vegors Jr., Nucl. Phys. **A252**, 260 (1975).
[28] U. Agvaanluvsan *et al.*, Phys. Rev. C **70**, 054611 (2004).
[29] C. Coceva, A. Brusegan, and C. van der Vorst, Nucl. Instrum. Methods Phys. Res. A **378**, 511 (1996).
[30] W. Gelletly *et al.*, J. Phys. G **11**, 1055 (1985).
[31] R. Firestone, private communication.
[32] S. F. Mughabghab *Neutron Cross Sections*, (Academic Press, New York, 1984), Vol. I, part B.
[33] E. Lipparini and S. Stringari, Phys. Rep. **175**, 103 (1989).
[34] J. Kopecky and R. E. Chrien, Nucl. Phys. **A468**, 285 (1987).
[35] J. Kopecky, M. Uhl, and R.E. Chrien, Phys. Rev. C **47**, 312 (1993).
[36] D. Frekers *et al.*, Phys. Lett. B **244**, 178 (1990).
[37] A. Schiller *et al.*, preprint nucl-ex/0011018.
[38] M. Krtička *et al.*, Phys. Rev. Lett. **92**, 172501 (2004).
[39] Y. Alhassid, G. F. Bertsch, and L. Fang, Phys. Rev. C **68**044322 (2003).
[40] A. Schiller *et al.*, Phys. Rev. C **68**, 054326 (2003).
[41] S. T. Boneva, V. A. Khitrov, A. M. Sukhovoj, and A. V. Vojnov, Nucl. Phys. **A589**, 293 (1995).
[42] S. T. Boneva *et al.*, Fiz. Elem. Chastits At. Yadra **22**, 479, 1433 (1991) [Sov. J. Part. Nucl. **22**, 232, 698 (1991)].
[43] P. P. Ember, T. Belgya, J. L. Weil, and G. Molnár, Ap-

plied Radiation and Isotopes **57**, 573 (2002).
[44] T. Belgya, *et al.*, in *Capture Gamma-Ray Spectroscopy and Related Topics*, Proceedings of the Eleventh International Symposium, Pruhonice near Prague, 2002, edited by J. Kvasil, P. Cejnar, and M. Krtička (World Scientific, New Jersey, 2003), p. 562.
[45] Data extracted using the NNDC on-line data service from the ENSDF database.
[46] R. Chankova, Ph.D. thesis, Oslo University, 2004 (in preparation).
[47] M. Guttormsen, *et al.*, J. Phys. G **29**, 263 (2003).
[48] L. Henden, L. Bergholt, M. Guttormsen, J. Rekstad, and T.S. Tveter, Nucl. Phys. **A589**, 249 (1995).
[49] M. Guttormsen, T. S. Tveter, L. Bergholt, F. Ingebretsen, and J. Rekstad, Nucl. Instrum. Methods Phys. Res. A **374**, 371 (1996).
[50] M. Guttormsen, T. Ramsøy, and J. Rekstad, Nucl. Instrum. Methods Phys. Res. A **255**, 518 (1987).
[51] J. Kopecky and M. Uhl, Phys. Rev. C **41**, 1941 (1990).
[52] T. von Egidy, H. H. Schmidt, and A. N. Behkami, Nucl. Phys. **A481**, 189 (1988).
[53] J. Dobaczewski, P. Magierski, W. Nazarewicz, W. Satuła, and Z. Szymański, Phys. Rev. C **63**, 024308 (2001).
[54] C. Fransen *et al.*, Phys. Rev. C **67**, 024307 (2003).
[55] C. Fransen *et al.*, Phys. Rev. C **70**, 044317 (2004).